PAN AFRICAN CRUSTAL SHORTENING FARTHER WEST IN THE CENTRAL EASTERN DESERT, EGYPT

Maher El Amawy[1], Basem Zoheir[1], Nesma Gamal[1] and Mohamed Abdel Wahed[2]

(1) *Department of Geology, Faculty of Science, Benha University.*

(2) *Department of Geology, Faculty of Science,Tanta University.*

ABSTRACT

The Neoproterozoic basement rocks of the Haggar Dungash area, Barramiya district, encompass ophiolitic assemblage of allochtonous blocks and clasts of serpentinite, metagabbro, metabasal and amphobolitest, which are tectonically embedded in highly sheared matrix of highly sheared ultramafic derivatives. This assemblage is separated from island arc volcanic/volcaniclastic rocks by oblique thrust and strike-slip faults, while discrete elongate bodies of gabbro-diorite and granitic intrusions occur along the axial planes of plunging anticlines and fault intersections.

Synthesis of the structural elements indicates three-fold deformational history (D_1, D_2 and D_3), which accompanied with two main shortening events; one major during D_2 followed by a local one during D_3. The earlier (D_1) is rare and preserved in the highly sheared ophiolitic derivatives and, sometimes, in the Island arc volcanics. D_1 fabrics include WNW-ESE foliation (S_1) and fold axes and WNW-ESE minor thrusts. Shortly, it was coeval with the initial stage of terrane accretion but their structural features are strongly superimposed by a later deformation (D_2). D_2 fabrics include abundant WNW-ESE to ~ E-W oblique thrust and WNW- to W- plunging folds. Transpression regime was recognized on the WNW-ESE strike-slip faults and related to the partitioning of deformation between sinistral shear and thrust component. D_3 Structures are the result of movement along Idfu-Marsa Alam dextral shear activated northward in the present area and reflected by the influence of F_3 overturned fold and parallel ENE-WSW dextral strike-slip fault.

Structural modeling shed light on the change from early ENE-WSW to E-W compressional regime into a late NNW-SSE shortening related to $\sigma 1$ rotation from ENE or ~E to NNW. The tight and overturned morphology of D_3 folds, together with the oblique movement on the WNW-ESE to ~E-W transpressive faults indicate a rather intense, non-coaxial or deformation via simple shear during the Pan-African orogeny. This regime is followed during D_3 by less intense, non-coaxial ENE-WSW dextral shear.

Key words: Pan African shortening, transpression regime, and Central Eastern Desert

1. INTRODUCTION

During the past two decades transpression involving oblique convergence has been utilized to explain the deformation kinematics in the Eastern Desert of Egypt (Loizenbauer et al., 2001; Makroum, 2001; Bregar et al., 2002; Fritz et al .,2002; Abd El Wahed, 2003; Makroum, 2003; Helmy et al.,2004 ; Shalaby et al., 2005; Abd El Wahed, 2007,2008; Abdeen et al., 2008; Abd El Wahed and Abu Anbar, 2009;Abd El Wahed, 2010; Shalaby, 2010). Transpression represents a characteristic feature of obliquely convergent mobile belts and involves a combination of pure shear and simple shear models to interpret structural

features within a narrow zone of deformation (Jones and Strachan, 2000; Woodcock and Rickards, 2003; Kim et al., 2004; Reddy and Occhipinti, 2004; Matin, 2006; Dehler et al., 2007; Abd El Wahed, 2008; Sarkarinejad et al., 2008; Goscombe and Gray, 2008; Abd El Wahed and Abu Anbar, 2008; Kumar and Parasannakumar, 2009; Johnston and Gutierrez Alonso, 2010; Karniol et al., 2008).

The present area is located farther west in the Central Eastern Desert including Umm Higlig and environs (Fig. 1). It represents the southern, eastern and northern continuations of Barramya, Abu Mireiwa and Mueilha areas respectively. El Ramly et al. (1993) considered the Central Eastern Desert as almost built up of ophiolitic mélange and associated rocks, accreted arcs together with subordinate molasses - type sediments, granitoids and late-tectonic volcanics. However, Moustafa and Abdalla 1954, El Ramly and Al Far 1955) classified these rocks as metamorphosed sediments, amphibolites, serpentinites and related rocks, gabrro – epidiorite-diorite-complex, granites and post granite dykes. Habib et al. (1986) studied Abu Mireiwa and classified the basement rocks into four rock units; ophiolites, flychiod metasediments, calc-alkaline metavolcanics and a basic layered intrusion. On the other hand, El Amawy (1997) classified the Pan African basement of Wadi Umm Higlig and environs into moderately to strongly deformed ophiolitic mélange that is made up of allochthonous blocks and fragments dominated by ophiolitic composition of ultramafic rocks, metagabbros, pillowed metabasalts and amphibolites together with metavolcanics. These rocks are incorporated inside a matrix of highly sheared ultrmafic derivatives and volcaniclastic metasediments. Totally, these rocks are intruded by syn-tectonic gabbros and, elsewhere, syn- tectonic granitoids.

Tectonic evolution of the Central Eastern Desert was early dealt with by Sabet et al. (1976) in which they subdivided this part, based on geosynclinal concept, into different blocks separated by deep-seated faults. Herein, the present area lies within Mueilha and Beizah blocks separated by E-W deep-seated fault. To the north, in Barramiya area, Abdel Khalik (1979) considered that folds represent one episode of folding and most of them are tight and plunged ENE. He distinguished also shear, thrust and strike slip faults along the E-W, ENE-WSW and NW-SE directions respectively. Other structural contributions were added also by El Gaby (1983) and El Gaby et al. (1988) who considered Idfu- Marsa Alam road as major right-lateral shear zone. Moreover, El Amawy (1991) and El Gaby (1994) concluded that the study area had been subjected to a principal stress from the NE direction. Initially, this stress is mostly subduction-related processes as confirmed from the strike of WNW-ESE thrust planes and vergence of F_1 axial planes in the WSW direction.

In the present study, field mapping using landsat images of different scales, petrography and structural analysis were carried out aiming at clarify the structural evolution and episodes of shortening of the Pan African rocks.

2. GEOLOGIC SETTING

The exposed Pan African basement rocks of the study area are classified from, bottom to top, into the following:

IV - Syn-tectonic granitoids
III -Syn-tectonic metagabbro-diorite
II - Island arc volcanic assemblage

-Volcaniclastic metasediments (metamorphosed agglomerate and tuffs)

- Highly sheared metavolcanics (Hb schist, epidote chlorite schist, chlorite schist with remnant of metabasalt)

I - Ophiolitic assemblage:

-**Matrix** (Talc tremolite schist, talc schist, graphite schist, talc carbonates (listvinite) and metasiltstone)

-**Blocks (**serpentinites and relics of ultramafics, ophiolitic metagabbros, highly deformed pillow lava and amphibolites)
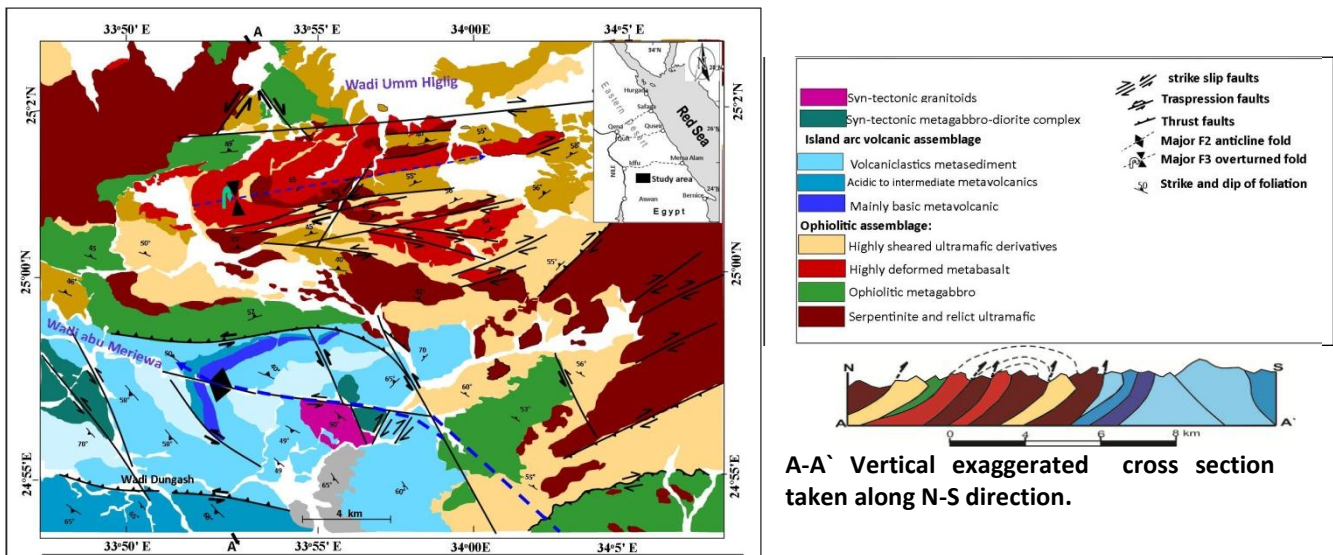

Fig. (1) Geologic map of the study area.

I- Ophiolitic assemblage

On the geologic map (Fig. 1), the ophiolitic assemblage of violet, green, red and yellowish brown colors cover the northern and eastern parts where island arc volcanic as blue and pale blue color occupy the central and western parts of the study area. The contacts in-between are oblique thrust or transpression deformations. The whole structure

Fig. (2) Field relationships at Umm Higlig and environs.(a) Remnants of basalt blocks in highly sheared ultramafic rocks; photo looking SW.(b)) Traces of graphite talc schist (blue arrows) in highly sheared ultramafic derivatives; Photo looking NW .(c) Pillowed metabasalt consisting of laths of plagioclase, orthopyroxene (enstatite) and small amounts of chlorite and quartz; CN, X2.0.06.(d) Amphibolite composed of hornblende, plagioclase and quaassociation with epidote, chlorite and actinolite; CN, X2.0.06.

was intruded by syn-tectonic metagabbro-diorite. The ophiolitc assemblage is markedly extensive in the present area and comprises Neoproterozoic allochthonous blocks (ultramafic rocks, metagabbros, pillow metabasalts and amphibolites). Tectonically, these blocks are incorporated within a matrix of highly sheared ultramafic derivatives.

The ultramafic rocks are classified into massive serpentinites (with relics of pyroxenite and dunite) and peripheries of highly sheared ultramafic derivatives; Talc tremolite schist, talc schist, graphite schist and talc carbonate (Figs. 2a-2b). Microscopically, the serpentinites are composed of antigorite, minor lizardite together with chrysotile and opaque of mainly chromite.

Ophiolitic metagabbros are less common, exposed between G. Hagar Dungash and Marwet Umm Higlig and crop out in the northern and south eastern parts of the mapped area. They form elongated masses against the matrix and, microscopically, they are fine-, medium- and coarse-grained and consist of plagioclase, actinolite and hornblende together with epidote and calcite. Accessories are iron oxides, ilmenite and sphene.

The highly sheared metabasalts are mainly exposed, in the northern part, at Wadi Umm Higlig forming the inner part of the major overturned fold. These rocks are tectonically enclosed within and stretched parallel to the main foliation. They are sheared and enclosed less distinct pillows and exposed, in the south western part, at Wadi Dungash forming the core of the major anticline (Figs. 1 and 2c). Microscopically, they are composed of plagioclase laths, actinolite, tremolite, epidote and chlorite with little amounts of quartz, sphene, calcite and iron oxides.

The amphibolites occur as very small detached fragments within the matrix and possess tectonic contacts against the surrounding rocks. Under the microscope, they are composed of hornblende, plagioclase and quartz with association with epidote, chlorite, sphene and iron oxide (Fig. 2d).

II-Island arc volcanic assemblage

The highly sheared metavolcanics are the next in abundance to the ultramafic rocks and represented by metabasalts, basaltic meta- andesites **(**Fig. 1). In the southeastern part of the mapped area, the metavolcanics are dominantly metabasalts but changes gradually westward into basaltic meta-andesite. Close to the ophiolite contact, they are highly deformed and transformed completely into hornblende schist, epidote chlorite schist, chlorite schist with remnant of metabasalt (Figs. 3a-3c).

The volcaniclastic metasediments occupy low-lying exposures north of Wadi Dungash and have intermediate to acidic composition. They range, in size, from ash to lapilli tuffs and, elsewhere, enclose thin bands of quartzite (Fig. 3d).

III- Syn-tectonic metagabbro-diorite

The syn-tectonic metagabbro-diorites are intruded into the pre-existing rocks. Microscopically, they are coarse-grained and composed of plagioclase, oxyhornblende with relics of augite and small amounts of quartz together with chlorite, iron oxides and sphene.

IV- Syn-tectonic granitoids

The syn-tectonic granitoids are mainly granodiorite in composition and occupy low relief terrains in the southwestern part of the mapped area. They show intrusive contacts,

spheroidal exfoliation structure and emphasize cataclasis along the shear zones. Microscopically, they consist of plagioclase, quartz, hornblende, rare biotite, and orthoclase with sphene and iron oxide.

Fig. (3) Field relationship of Umm Higlig and Environs (a) Steeply dipping hornblende schist; Photo looking NW. (b) relics of trachytic texture preserved in metavolcanics. Note amphibole (brown color) altered to carbonate and epidote; CN, 2.0.06. (c) Epidote chlorite schist; CN, 2.0.0). (d) Dashed line refers to foreign pebbles in agglomerate; Photo looking SW.

3. Structural analysis
3.1. Ductile structural deformations
3.1.1. Foliations

The study area exhibits three foliation trends pertaining to three phases of foliations (S_1, S_2 and S_3). These phases are related to D_1, D_2 and D_3. The first phase S_1 foliation is essentially axial planar with F_1 folds, penetrative and mostly striking WNW-ESE. S_1 dips 30°- 45° NE and, elsewhere, exhibits steeper dips (50° - 60°) towards the SW. In general, it is parallel to S_o bedding planes in the volcaniclastic metasediments and, sometimes, to shearing foliation S_{sh} developed between the thrust slices of the ultramafic rocks and the underlying arc volcanic assemblage.

The second phase S_2 foliation is a crenulation foliation and non - penetrative. It is axial planar to F_2 folds, striking NW-SE and generally dipping at moderate angles (50° - 65°) to NE and, in places, SW S_3 foliation is mainly crenulation foliation and axial planar to F_3 minor folds and commonly striking ENE-WSW to NE-SW. The foliation is non- penetrative, axial planar to F_3 major overturned fold and striking ENE-WSW as well as dipping at moderate and steep angles ($55°$ - $70°$)

3.1.2. Lineations

Lineations are distinctive and related to the first, second and third phase of deformations. Commonly, they include crenulation lineation, pencil-like lineation and kinking axes, pinch and swell structures. L_1 lineation is formed during D_1, coaxial with F_1 minor fold axes and gently plunged WNW and, in some cases, NW, SE and ESE. L_2 lineation is resulted by D_2, parallel to F_2 folding axes and plunge moderately NW, but in places SE. L_3 lineation is related to D_3, parallel to the axes of F_3 folds and steeply plunged ENE and, in places, WSW.

3.1.3. Folds

Structurally, folds in the study area are differentiated into minor and major folds. Totally, they are recognized into three phases of F_1, F_2 and F_3 folds. F_1 folds are mainly minor, formed during D_1 and frequently involved within the limbs of the major folds. They vary in style from very tight, intrafolial, overturned, asymmetric, symmetric, disharmonic to chevron ones. F_1 folds are oriented WNW-ESE to NW-SE and commonly plunge at gentle angles towards NW, WNW and, sometimes, ESE and SE. Commonly, they are preserved in the highly sheared ophiolitic sequence and volcaniclastic metasediments. Field observations revealed that the F_1 minor folds are axial planar to minor thrusts and, elsewhere, coaxial with the F_2 major anticlinal fold indicating that they were affected, in part, by D_2 deformation.

Major folds are observed in the geologic map (Fig. 1); one in the southwestern part and is represented by anticlinal fold and another to the north denoting F_3 phase of folding. F_2 southwestern major anticline was formed during D_2 and involved in the arc volcanic assemblage. Its axis starts in the east along NW-SE then turns to the west alongside WNW-ESE to E-W trends, which deciphers a new episode of folding in NE direction. It is bounded from the north northeastern side by transpressive and major strike-slip faults. The fold is tight and its axis extends for a distance of 10 km and generally plunges WNW. The axial plane strikes NW–SE to WNW–ESE and dips steeply NNE to NE. Its northeastern limb dips at an angle (40° -55°) whereas the south southwestern limb is steeper (65° - 70°). Others of F_2 folds are minor and developed within the limbs of F_2 major fold and with style of overturned, less tight and asymmetric varieties.

The second major fold is recognized in the northern part of the mapped area affecting the ophiolitic assemblage and represents the phase of F_3 fold (Fig. 1). It was formed through the extremely ductile rotation of the ophiolitic components in the matrix and volcanclastic metasediments during the third phase of folding. The fold is less tight and its axial trace extends for about 8km or even more. It strikes ENE–WSW and moderately plunges ENE. The northern limb of this fold is horizontally displaced eastward along ENE–WSW fault and mostly formed of massive ultramafic rocks and sparsed hillocks of ophiolitic gabbroic rocks. Therefore, the attitude of fabric elements within this limb is somewhat limited. The fold is cored by metagabbros, pillow metabasalts and matrix of highly sheared ultramafic derivatives and volcaniclastic metasediments but flanked to the south by high relief ultramafic rocks. Others of F_3 minor folds are well recognized in the northern and, elsewhere, in the central parts of the study area. Commonly, they are distinctive with open styles and their axes follow the NE-SW to ENE-WSW directions and plunge steeply ENE and NE, in some places, SW and WSW.
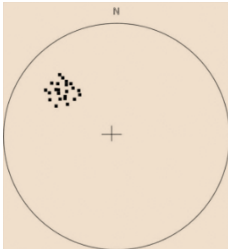
3.1.4. Geometrical analysis

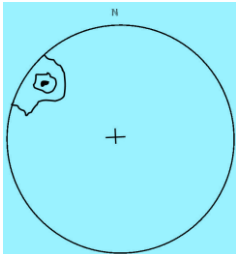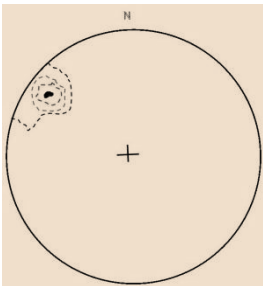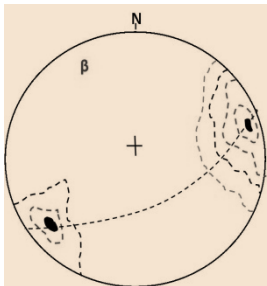Field reading taken for the different structural elements (including foliation, lineation and axes of minor F1 and F2 folds) are projected on the lower hemisphere of Schmidt's equal area net (Fig. 4).

3.1.5. Folds analysis

F1 folds are frequently included within the limbs of the major folds. They are represented as minor and kink axes (L_o // L1). L_1 lineation is few in numbers. L1 lineation indicates concentration plunging 20° on a bearing N65°W. β1 is determined by maximum concentration of L1 lineation (β1=L1).

In Figure (Fig. 4), the north to northwestern limb represents a subarea of F2 major

anticlinal folds located in southwestern part and affecting the highly sheared ultramafic derivatives and island arc assemblage. The poles to S2 foliation exhibit great girdle patterns and are nearly coaxial with the maximum concentration of L2 lineation and the axes of F2 minor folds. The center of maximum concentration of L2 lineation attains plunging 28° N70°W and 30° N65°W. Within the south to southwestern limb of this F_2 major anticlinal fold, S2 foliations are widespread and their poles form great circle patterns for their poles (β2). L2 lineation indicates concentrations plunging 30°on a bearing N65°W and 33°on bearing N38°W. Within this major fold, the readings of S3 foliations are widespread and their poles form great circle patterns. The orientation diagrams for L3 lineation define a maximum concentration within small field plunging 54° N 50 °E and 53°N 35°E. Statistically, β1 and β2 are to great extent coaxial with the maximum concentrations of L1 and L2 lineations. F_3 major fold located farther north of the mapped area (Figs. 1). S1 and S2 foliations are few in number and insufficient for geometric analysis. L1 and L2 lineations are insufficient also for representation. L3 lineation indicates concentrations plunging 45°on a bearing N60°E and 42°on a bearing N55°E.

Phase of def.	Structural elements			
	L_1			
D_1	Lineation N=42 0,5,10,15,20 %		Lineation N=42 0,5,10,15,20 %	
	L_2		**S_2**	
D_2	Lineation N=72 0,5,10,15,20 %		Foliation N=95 0,5,10,15,20 %	
	F_2 major anticline fold			
	NW limb		SE limb	Synoptic diagram

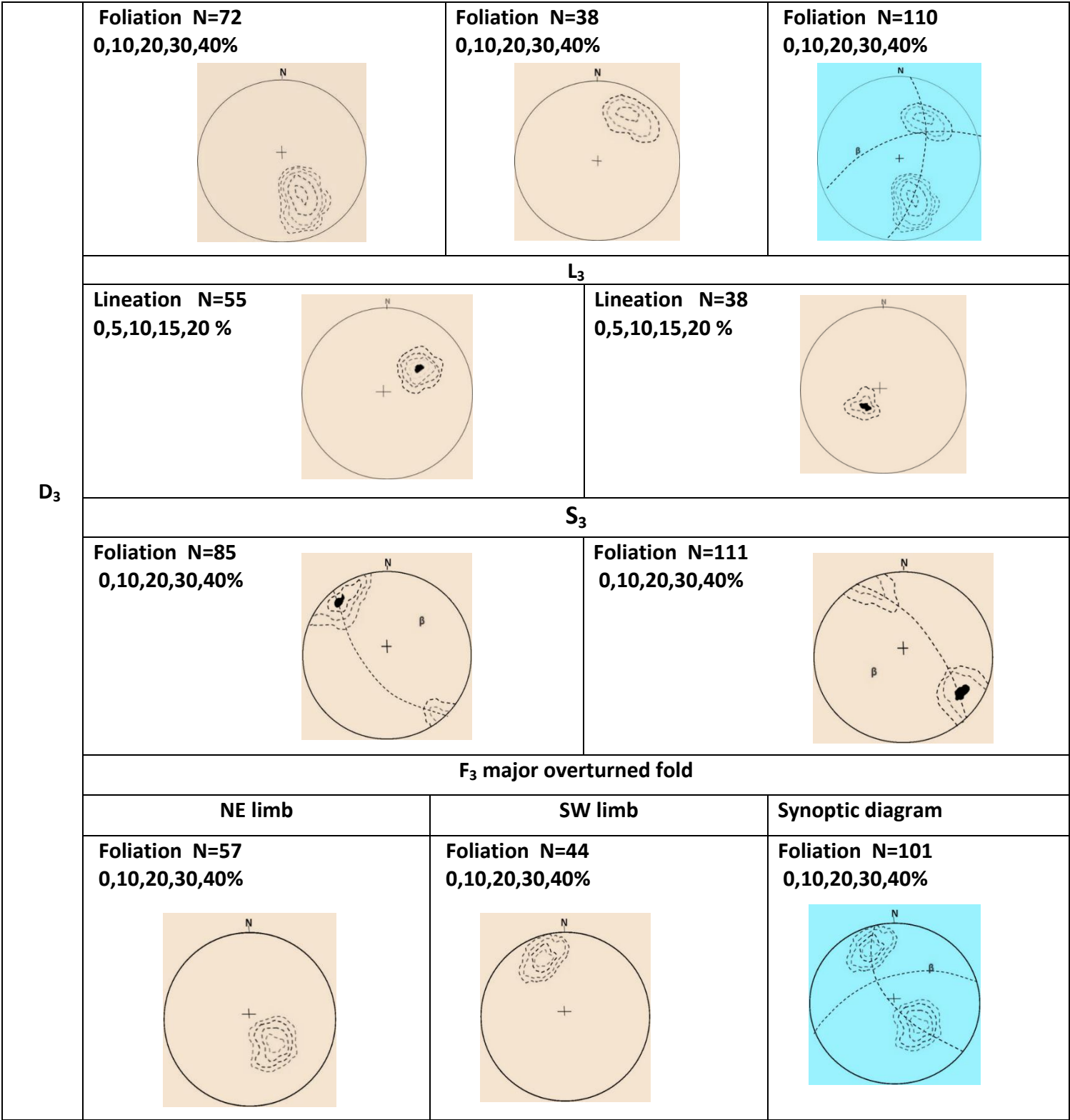|	Foliation N=72 0,10,20,30,40%	Foliation N=38 0,10,20,30,40%	Foliation N=110 0,10,20,30,40%
D_3		**L_3**	
	Lineation N=55 0,5,10,15,20 %	Lineation N=38 0,5,10,15,20 %	
		S_3	
	Foliation N=85 0,10,20,30,40%	Foliation N=111 0,10,20,30,40%	
		F_3 major overturned fold	
	NE limb	**SW limb**	**Synoptic diagram**
	Foliation N=57 0,10,20,30,40%	Foliation N=44 0,10,20,30,40%	Foliation N=101 0,10,20,30,40%

Fig. (6) Equal area lower hemisphere diagrams showing stereonets plotted for F_1 minor folding axes, L_1 lineation and the foliation on the limbs of F_2 and F_3 major folds developed during D_1, D_2 and D_3 respectively.

3.2. Brittle structural deformations

3.2.1. Thrust and transprssive faults

Faults observed in the study area are the most characteristic elements of brittle deformation. They have mainly WNW-ESE, ENE-WSW, NW-SE and NE-SW orientations. The WNW-ESE fault trend embraces the transpression faults (i.e. oblique convergent faults) and is represented, at the central part of the study area, by two faults. Both faults brought the hanging wall of ultramafic rocks, at sinistral oblique movement, against the footwall arc volcanic assemblage. This movement is documented by strong shearing, alignment of disconnected talc lenses and coexistence of subhorizontal with subvertical stretching striations along and on the fault planes. The planes of these faults are planar to F_2 major folds and dip N to NNE at angles 40°-55°. The first fault defines the northern part of F_2 major anticline. It starts in the east as a branch of a main NW-SE sinistral strike-slip fault and extends throughout the area for a distance of more than 12km then conceals blindly farther west beneath the ophiolitic and arc volcanic assemblages. The association of subhorizontal and subvertical striations noted along this fault reveals partitioning of simple and pure shears. In this case, the bulk strain is resolved into two displacements; one is accommodated with simple shear (sinistral strike-slip component) with other of pure shear (thrust component) leading at the end to sinistral oblique convergence regime or transpression. As the present fault is a branch of the main NW-SE sinistral strike-slip, this means a transformation of the sinistral shear (pure wrenching) on the main NW-SE fault into a combination of sinistral shear with oblique shear (convergent wrenching) on the WNW-ESE transpression fault. This assumes operation of sinistral tectonic transport of the ophiolitic assemblage along the main NW-SE sinistral strke-slip fault then association of this transport by pure shear component resulting in west to west-southwest directed thrusting.

The second fault is located south of the first fault and delimits the termination of south to southwestern limb of F_2 major anticline. It extends for about 11km or even more. It defines the contact between the highly sheared volcaniclastic metasediments with unmappable slices of ophiolitic rocks against the underlying metavolcanics. Its contact is characterized with the same properties as the first fault. Of prime interest, some of F_1 minor folds are axial planar to the planes of the F_2 major faults, however field observation showed development of NW-SE to WNW-ESE minor thrusts between the major transpression faults and, elsewhere, along minor intrafolial, overturned and isoclinal F_1 folds. On the planes of these minor thrusts, nearly vertical stretched striations were developed and recognize mostly a kinematic indicator of pure shear. This assumes association of pure thrusts; at least, during the early stage of deformation (D_1) and the development of some F_1 minor folds were consistent with these thrusts.
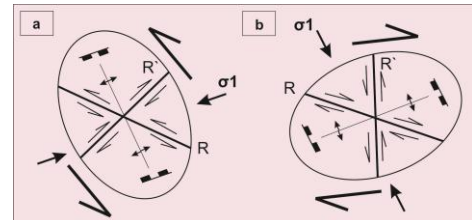
3.2.2. Strike-slip faults

The strike slip faults represent the main factor of brittle structures dissecting all rock units, most of the preceding D_1 and, elsewhere, D_2 structures in two main categories; one striking NW-SE and other with strike ENE-WSW. The first category affects mainly the southern two-third of the mapped area, whereas the influence by second category is markedly observed in the northern part (Fig. 1).

The NW-SE strike-slip faults range in length between some meters to km-scales and are characterized by sinistral shear. As the trend of these faults attain the strike NW-SE, their

planes show subhorizontal striations and are dominated by high angle of dip ($65°$-$80°$) in the NE direction. When the fault planes swing and constrain along WNW-ESE trend, the values of dip become gentle to moderate (about $30°$-$55°$) and the subhorizontal striations are associated with subvertical ones. This reveals that as the strike of these faults turns WNW-ESE, the sinistral strke-slip movement is accompanied with thrust-slip. In general, the NW-SE faults separate between the ophiolitic rocks and the arc volcanic assemblage. They show alignment of strong shearing and cataclasis, talc lenses, wavy anastomosing surface in the highly sheared ultramafic derivatives. Cataclasis is also noted in the syn- tectonic metagabbro exposed along the NW-SE faults further west southwest. Their planes are mostly planar to the axial planes of F_2 folds and, in places, F_1 folds. Field observations and analysis along the NW-SE fault trends showed inconsistent crosscutting interrelationship between common array of WNW-ESE and rare array of NE-SW faults, where faults of the first array displace the other trends of the second array and vice versa. This pattern summarizes, most probably, the WNW-ESE and NE-SW fault trends represent segments of sinistral Reidel and conjugate dextral Reidel shears (R and R′ shears), which were created and enhanced via the displacement along the main shear of NW-SE sinistral strike-slip faults. This assumes an acting principal stress from ENE to nearly E direction (Fig. 5a).

Fig. (5) Proposed models to illustrate the structural relationship between the WNW-ESE and NE-SW to ENE-WSW developed on the main NW-SE sinistral fault trends (a) and those NW-SE and NNE-SSW fault trends developed within the ENE-WSW major dextral strike-slip fault (b).

Faults of second category (i.e. ENE-WSW faults trends) displace the NW-SE faults, S_1 and S_2 foliations and the axial traces of F_1 and F_2 folds. The faults show remarkable dextral sense of horizontal displacement that reaches up to 1200 m. Their planes are mostly planar to F_3 folds (ENE-WSW trend, in particular) and dip $75°$-$85°$ WNW to NW and, sometimes, ESE to SE. Generally, they show strong shearing in the ultramafic and metavolcanic rocks. Further northward, ENE-WSW major fault trend of this category is recognized bounding the major F_3 synclinal fold in the ophiolitic rocks. This fault runs for about 16 km then terminates beyond the present area in the east northeast direction. It is, more or less, parallel to Idfu-Marsa Alam shear zone (about 4km to the north of the study area) and along it the northern flank of F_3 major syncline is forced past its southern one to the east. Kinematic indicators noted along this fault showed two smaller segments of WNW-ESE Reidel and NNE-SSW conjugate Reidel shears cut across the main trend of this fault suggestive an acting principal stress along the NNW-SSE trend (Fig. 5b).

To sum up, the proposed models carried out for illustration the relationship between the different structural patterns of F_1, F_2, F_3 folds with the associated categories of NW-SE and ENE-WSW faults (Fig. 5), elucidate a change from early ENE-WSW compressional regime into a late NNW-SSE shortening. This means rotation of σ1 rotation from ENE to NNW. In other words, the tight and overturned morphology of D_2 folds together with the oblique movement on the WNW-ESE faults indicate intense, non-coaxial NW-SE sinistral regime. This regime is followed during D_3 (further northward, in particular) by less intense, non-coaxial ENE-WSW dextral shear (Fig. 5).

Discussion and conclusions

In general, the shear zones in the Eastern Desert are delineated within and between the low grade suprastructure and high infrastructural domains and document substantial tectonic transport (or shortening) during the Pan African orogeny (900-600 Ma). Earlier tectonic transport was generally towards the W, WSW to SW and acted by pure shear and principal stress from the E, ENE to NE or even NNE (El Gaby et al., 1988, 1994; Abdel Khalek et al., 1992; Fritz et al., 1996; Noweir et al., 1996; El Amawy, 1999, 2001, and Mansour et al., 1999). This is succeeded later by a transport direction in the NW (Noweir et al., 1996, and El Amawy, 2001). However, mechanism of movement by pure or simple shears or a combination of both is still under debate. Some authors (i.e. El Gaby et al., 1988 and 1994, Abdel Khalek et al., 1992; Noweir et al., 1996, and El Amawy, 2001) evidenced the early transport and its deformation due to pure shear and attributed this from the crosscutting relationships of pure thrusts by strike-slip faults, the vergence of folds and domes and orientation of the subvertical stretching lineation in the direction of tectonic transport with the attitudes of folding axes and thrusts as their traces are orthogonal to this transport. Despite this, El Gaby et al. (1988, 1994 and 1996) assumed pure and simple shears during this early tectonic transport (i.e. compressional or thrusting contemporaneous with strike slip faulting) indicative a transpression regime. In contrast, this is comparable only in the late stage of tectonic transport, which induced bending of the pre-existing folding axes and thrusts, as well as sinistral shearing, divergence (transtension) and convergence (transpression) sites along Wadi Allaqi (El Amawy, 2001 and El Amawy et al., 2002). At time interval 615-600 Ma, Berth et al. (1994) recognized a transistional period of compressional and extensional tectonic phases, which is approximately synchronous with the period activity of Najd fault system (620-540 Ma, Stern 1985) that extends from Saudi Arabia to the Central Eastern Desert of Egypt and represents an important stage of the association of transtensional and transpressional tectonics along NW-SE sinistral shear.

Following studies, in the Central Eastern Desert, confirmed the NW to WNW tectonic transport along NW-SE parallel Najd fault system and in mechanism of simple shear, where the sinistral shear component was associated with dip-slip component and, elsewhere with reverse component forming transtensional and transpressional tectonics (Fritz et al. 2002, Makroum 2001 and 2003, Abdeen and Greiling 2005, Abd El-Wahed 2007, 2008 and 2010, Fowler et al. 2007, Abd El-Wahed and Kamh 2010).

On the landsat image (Fig. 6), Hafafit area is the most conspicuous part of a larger scale antiformal infrastructural domain in the Central Eastern Desert, where various gneisses are exposed beneath low grade subrastructural of ophiolite-arc volcanics succession. The gneisses represent suite of the oldest or old continental crust (Abdel Khalek and Abdel Wahed, 1988; El Gaby et al., 1988, 1994 and 1996, and Akaad, 1996) or igneous rocks of ocean floor and volcanic arc characteristics and related metasediments, together with metasedimentary units derived from a pre Pan African source area (Rashwan, 1991; El Ramly et al., 1993; Greiling el al., 1994, and Fowler et al., 1999). The Hafafit area is dominated by NW- to NNW- trending low angle thrusts and faulting and the thrusts are linked to floor and roof thrusts (e.g. Abdel Khalek and Abdel Wahed, 1988; El Ramly et al., 1993, and Greiling et al., 1993). Therefore, the gneissic units form an antiformal stack beneath the overlying low grade successions. Kinematic indicators (e.g. stretching lineation) show compression in a NW-SE direction (Greiling et al., 1993 and 1994). This explains a

transport direction parallel to the strike of thrusts, nevertheless these authors didn't refer whether the thrusts are strike slip linked faults or not. Fowler et al. (1999) confirmed the general NW transport but added that it was accompanied by granitoid intrusions and followed later by a SW-ward thrusting event producing the doming in the central part of Wadi Hafafit Culmination. This explains a combination of the NW-trending transport at the late stage of deformation by SW-thrusting, and consequently oblique convergence or transpression? The common subhorizontal NW-trending stretching lineation noted on the major thrust (Nugrus thrust; El Ramly et al., 1993, and Greiling et al., 1993), running parallel to the Hafafit Culmination, is parallel to the NW-SE sinistral Najd fault system. Kinematically, this reveals that the Nugrus thrust fault is related to the sinistral Najd system. On the other hand, Abd El-Wahed and Kamh (2010) extended their view to relate the deformation along Nugrus shear zone to NW–SE sinistral strike-slip movement and formation of F_1 tight to isoclinal non-cylindrical folds and thrust fan as a consequence of transpression. Northward, the strike of NW-SE Nugrus sinistral strike-slip fault changes its orientation to bifurcate, in the present area (about 60 km NW of Hafafit area), along the WNW-ESE to NW-SE, E-W sinistral and NE-SW dextral strike-slip trends (Fig. 6).

Detailed structural analysis, in the present area, emphasized three phases of deformations (D_1, D_2 and D_3). D_1 structures are documented in the highly sheared ophiolites and rarely in the island arc volcanics. They are represented by F_1 minor tight, intrafolial, recumbent, isoclinal folds and, sometimes, WNW-ESE striking minor scale thrusts. Subvertical striations noted along the earlier NW-SE to WNW-WSW minor thrusts indicate pure shear due to a principle stress acting from the NE direction.

D_2 represents a major progressive phase of deformation along NW-SE strike-slip faults, where the movement was initiated with sinistral shear then accompanied, in places, with thrust motion (transition from wrenching stage to convergent wrenching or transpression regime) and the horizontal principal stress is rotated to act along ENE-WSW to E-W direction. D_2 structures are mainly NW-SE sinistral strike-slip fault trends, represented by transpression regime or oblique thrusts along the WNW-WSW sinistral faults, NW-SW to WNW-ESE transpressive faults and WNW-ESE trending F_2 major fold with others of F_2 minor folds. The NNE-SSW to NE-SW strike-slip fault trends represent secondary array of conjugated Riedel shear along the NW-SE strike-slip faults and, elsewhere, they are characterized with dextral transpression movement along their planes.

Fig. (6) Landsat image along Wadi Nugrus shear zone showing major structures and ellipsoid stresses (modified after Klitzch et al., 1987; Akaad et al., 1993, Fertiz et al., 1996 and 2002; Abd El Wahed and Kamh, 2010). Area labeled (a) in the key map is the study area.

D$_3$ structures are mainly recognized in the north and northeast, where the present area is located very close to the E-W Idfu-Marsa Alam dextral shear zone (Fig. 7). F$_3$ major overturned fold represents one of spectacular feature in the north affecting the ophiolitic assemblage and formed through the extremely ductile rotation of the ophiolitic component in the matrix and volcaniclastic metasediments during the third phase of folding. The fold is less tight and strikes ENE–WSW and moderately plunges ENE. The attitude of F$_3$ major fold and parallel ENE-WSW dextral fault shed light on the influence by Idfu-Marsa Alam shear zone and meanwhile assumes a directed stress from the NNW-SSW.

In conclusion, the present area is located within two phases of shortening; one along ENE-WSW to E-W and another along NNW- SSE to NW-SE. Structural modeling shed light on the change from earlier ENE-WSW to E-W compressional regime into a late NNW-SSE shortening, which was most likely due to σ1 rotation from ENE or ~E to NNW. The tight and overturned morphology of D$_3$ folds, together with the oblique movement on the NW-SE to WNW-ESE to transpressive faults indicate a rather intense, non-coaxial or deformation via simple shear during the Pan-African orogeny. This regime is followed during D$_3$ (further northward, in particular) by less intense, non-coaxial ENE-WSW dextral shear.

REFERENCES

Abdel Khalik, M.L. 1979. Tectonic evolution of the basement rocks in the Southern and Central Eastern Desert of Egypt. Bullins. Appl. Geol., King Abdul aziz Univ., Jedddah 3(1), 53-62.

Abd El-Wahed, M.A., 2007. Pan African strike slip tectonic of Wadi El-Dabbah Area. North Sibai core complex, Central Eastern Desert, Egypt. Annals of the Egyptian Geological Survey 29, 1-3.

Abd El-Wahed, M.A., 2008. Thrusting and transpressional shearing in the Pan-African nappe southwest El-Sibai core complex, Central Eastern Desert, Egypt. Journal of African Earth Sciences 50, 16–36.

Abd El-Wahed, M.A., Abu Anbar, M.M., 2009. Syn -oblique convergent and extensional deformation and metamorphism in the Neoproterozoic rocks along Wadi Fatira shear zone, Northern Eastern Desert, Egypt. Arabian Journal of Geosciences 2, 29–52.

Abd El-Wahed, M.A., S.Z. Kamh., 2010. Pan African dextral transpressive duplex and flower structure, Central Eastern Desert, Egypt. Gondwana Reserch. No of page 22.

Abdeen, M.M., Sadek, M.F., Greiling, R.O., 2008. Thrusting and multiple folding in the Neoproterozoic Pan-African basement of Wadi Hodein area, south Eastern Desert. Egypt Journal of African Earth Sciences 52, 21–2

Akaad, M.K., El Ramly, M.F., 1963. The Cataclastic–mylonitic gneisses north of Gebel El-Mayyit and origin of the granite of Shaitian type. Geological Survey of Egypt, Paper, No. 26. 14pp.

El Amawy, M.A., 1991. Structural and tectonic development of Wadi Bitan - Wadi Rahaba area, South Eastern Desert. Scientific Journal of Fac. Of Sci., Menoufia Univ., 5, 293 - 334.

El-Gaby, **S., 1983.** Architecture of the Egyptian basement complex, Proceeding 5th. international conference of basement tectonics, Cairo. El-Gaby, S., 1994. Geologic and tectonic framework of the Pan-African orogenic belt in Egypt, Proceeding 2nd.

International Conference of Geology of the Arab World, Cairo University, Cairo, Egypt, pp. 3-17.

El- Gaby, S., List, F.K., Tehrani, R., 1988. Geology, evolution and metallogenesis of the Pan African belt in Egypt. In: S.

El- Ramly, M.F., Al Far, D.M., 1955. Geology of El Mueilha – Dunash district .Geol.Surv.Egypt.44P.

El-Ramly, M.F., Ivanov, S.S. and Kochin, G.G., 1970. The occurrence of gold in the Eastern Desert of Egypt. In: O. Mohamed, M.F. Egypt, Cairo, pp. 53-64.

El-Ramly, M.F., Soliman, F.A., Rasmay, A.H. and Abu El farah, M. H., 1998. Petrographic and geochemical characteristics of the island arc volcanic rocks in the area between Wadi Gerf and Wadi Urn Khariga, Central Eastern Desert of Egypt. Annals of the Geological Survey of Egypt, 21: 1-22.

El-Ramly, M.F., Greiling, R.O., Rashwan, A.A. and Rasmy, A.H., 1993. Explanatory note accompany the geological and structural maps of Wadi Hafafit area, Eastern Desert of Egypt. Geol. Surv. Egypt 68, 53

Fritz, H., Dalmeyer, D.R., Wallbrecher, E., Loizenbauer, J., Hoinkes, G., Neumayr, P., Khudeir, A.A., 2002. Neoproterozoic tectonothermal evolution of the Central Eastern Desert, Egypt: a slow velocity tectonic process of core complex exhumation. Journal of African Earth Sciences 34, 543–576.

Habib, M.E., Hassan, M.A., Hashad, A.H., Abu Ela, E.F., 1987. Abu Mireiwa ophiolitic mélange west of Marsa Alam, Egypt. Bull Fac. Sci., Assiut Univ., 16(1-C), 139-197.

Hamimi, Z., El Amawy, M.A., Wetait, M. 1994. Geology and structural evolution of El Shalul dome and environs, Central Eastern Desert. Jour Geol., 38 (2), 575-595.

Helmy, H., Kaindl, R., Fritz, H., Loizenbauer, J., 2004. The Sukari Gold Mine, Eastern Desert, Egypt: structural setting, mineralogy and fluid inclusion study. Mineralium Deposite 39, 495–511.

Johnson, P.R. and Woldehaimanot, B., 2003. Development of the Arabian-Nubian Shield: perspective on accretion and deformation in the northern East Africa Orogen and the assembly of Gondwana. In: M. Yoshida, S. Dasgupta and B. Windley (Editors), Proterozoic East Gondwana: Supercontinent assembly and breakup. Geological Society of London, London, pp. 289-325.

Khalil, I.K., Helba, H.A., Mucke, A., 2003. Genesis of the gold mineralization at the Dungash gold mine area, Eastern Desert, Egypt: a mineralogical–microchemical study. Journal of African Earth Sciences V. 37, P. 111–122.

Kusky, T.M., Abdelsalam, M.G., Tucker, RD. and Stem, RJ., 2003.Evolution of the East African and related orogens, and the assembly of Gondwana. Precambrian Research, 123(2-4): 81-85.

Loizenbauer, J., Wallbrecher, E., Fntz, H., Neumayr, P., Khudeir, A. A., Kloetzil, U., 2001.Structural geology, single zircon ages and fluid inclusion studies of the Meatiq metamorphic core complex. Implications for Neoproterozoic tectonics in the Eastern Desert of Egypt. Precambrian Research 110, 357–383.

Makroum, F.M., 2001. Pan-African tectonic evolution of the Wadi El Mayit Area and its Environs, Central Eastern Desert, Egypt. The Second International Conference on the Geology of Africa, Assiut University, Egypt, 2, pp. 219–233.

Makroum, F.M., 2003. Lattice preferred orientation (LPO) study of the orogen-parallel Wadi Nugrus and Wadi Um Nar shears. Eastern Desert–Egypt using EBSD-technique. The

Third International Conference on the Geology of Africa, Assiut University, Egypt, 1, pp. 213–232.

Moustafa, G.A., Abdalla, A.M., 1954.Geology of Abu Mireiwa district. Geol. Surv., Egypt, 27P.

Noweir, A.M., El Amawy, M.A., Rashwan, A.A., Abddel Aziz, A.M., 1996. Geology and Structural evolution of the Pan African basement rocks around Wadi Umm Araka Norhern Wadi Allaqi, South Eastern DesertEgypt. Egypt .Jour of geology 40 (2), 477-512.

Ries, Ae., Shackleton, R.M., Graham, R.H. and Fitches, W.R., 1983. Pan-African structures, ophiolites and melange in the Eastern Desert of Egypt: a traverse at 26° N. Journal of the Geological Society, 140(1): 75-95.

Stern, R.J., 1994. Arc assembly and continental collision in the Neoproterozoic East African Orogen implications for the consolidation of Gondwana land. Annual Review of Earth and Planetary Sciences v. 22, p. 319–351.

Woodcock, N.H., Rickards , B., 2003. Transpressive duplex and flower structure: Dent Fault System, NW England. Journal of Structural Geology 25, 1981–1992.

الملخص العربى

اظهرت الدراسه الجولوجيه وجود وحدات معقد الخليط الأوفيوليتى ممثله بصخور الفوق مافيه ، الجابروالمتحول، البازلت الوسائدى المتحول، الأمفيبوليت بالاضافه الى البركانيات المتحوله. هذه الصخور توجد مدمجه تكتونيا داخل الانواع التهشيميه للصخور الفوق مافيه، الرسوبيات المتحوله والصخور الطفليه المتحوله.وتتباين العلاقه بين هذه الصخور جميعا من خلال المشاهده الحقليه .تظهر هذه الصخور ايضا تداخلات من صخور الجابر والجرانيت التكتونى المتزامن واخيرا بعض كتل صغيره من الجرانيت والجابر والتكتونى المتأخر.هذه الى جانب تأثر المنطقه ببعض الجدد فى اتجاه غرب شمنال غرب، شرق شمال شرق وشمال شرق.

ومن تحليل العناصر البنائيه اتضح ان المنطقه قد تعرضت الى ثلاث مراحل من التشوه أظهرت خلالهما انواع مختلفه من الطى، التورق، التخطط الى جانب صدوع الدسر، صدوع الضغط الانتقالى وصدوع الانزلاق المضربى. ومن تحليل قياسات صدوع الضغط الانتقالى والانزلاق المضربى وكذلك شكل طيات مرحلة التشوه الأولى والثانية والثالثة وصدوع الدسر أمكن ملاحظة أن المنطقه قد تعرضت اثناء حركة التجبل الافريقى الى ضغط من اتجاه شرق شمال شرق — غرب جنوب غرب الى تقريبا شرق - غرب ثم من الشمال الغربي الي الجنوب الشرقي.